

## Cold Atom Beam Splitter Realized with Two Crossing Dipole Guides

Olivier Houde, Demascoth Kadio, and Laurence Pruvost

*Laboratoire Aimé Cotton, CNRS II, bâtiment 505, Campus d'Orsay, 91405 Orsay cedex, France*

(Received 9 May 2000)

Cold rubidium atoms, coupled and guided in a vertical laser beam by the dipole force, have been split into two atomic beams, by using a second time-dependent laser beam crossing the vertical one at a 0.12 rad angle. Transfer efficiency as large as 40% has been obtained. At 10 mm below the cold atom source, the two atomic beams have a few hundred micron size and are more than one millimeter apart from each other.

PACS numbers: 32.80.-t, 03.75.Be

With the considerable progress realized in laser cooling techniques for ten years, many new fields are now explored, such as atom optics and atom interferometry [1,2]. These developments require reliable optical elements, such as lenses, atomic mirrors, or atomic beam splitters.

One of the most important goals is the realization of atomic beam splitters combining both a large efficiency and a large deviation angle, allowing large enclosed areas atomic interferometers. Experimental realizations of atomic beam splitters have been done. For most of them, they deal with only one of the two requirements. Many of the beam splitters use the momentum transfer, which occurs during a resonant atom-laser interaction. From one up to 140 photon momenta have been transferred to atoms along the laser direction [3–7]. Nevertheless, with a laser beam orthogonal to the atomic beam, deviations of only some ten milliradians angle have been achieved in these experiments. With such angles the interferometer areas are limited, except if large apparatus are used [8]. Bragg diffraction by an optical standing wave is another powerful method which provides a coherent splitting of atomic beams. Large angles have been obtained with many-orders Bragg diffraction or with very slow atoms [9–12]. Magnetic interactions lead also to the realization of large angle beam splitters—for example, by using a Y-shaped current carrying wire [13] or a concave corrugated magnetic reflector [14]. These methods are, however, restricted to nonzero magnetic momentum atomic levels.

In this paper we report on an atomic beam splitter which uses a far off-resonant atom-laser interaction. Our cold-atom beam splitter consists of two crossing dipole guides, one along the vertical direction, the other one along an oblique direction at an angle 0.12 rad from the vertical. Combining the splitting and guiding effects we generate two collimated beams. We demonstrate a large coupling efficiency and a splitting which reaches the millimeter range. Such a beam splitter is applicable to all atomic species and offers the flexibility of rearranging the laser beams externally to the vacuum chamber.

The atoms first enter the vertical guide. Although they are falling, they oscillate in the two-dimensional potential well created by the vertical guide. When the oblique guide

is on they see a modified potential: two wells, one due to the vertical guide and the other one due to the oblique guide. The overlap region of the two wells is the region where the atoms, initially inside the vertical guide, can pass into the oblique guide. To allow this atom transfer the atoms must oscillate at least once along this region. That condition and the well overlap determine the transfer efficiency.

The apparatus consists of an ultrahigh vacuum chamber in which  $^{87}\text{Rb}$  atoms are trapped and cooled in a magneto-optical trap (MOT) (Fig. 1). The magnetic field gradient is 14 G/cm at the chamber center. The trapping laser beams are provided by three laser diodes. A 5 mW narrow linewidth master laser injects a 50 mW diode laser, providing the trapping beam. Its frequency is tuned near the  $5S_{1/2}F=2 \rightarrow 5P_{3/2}F'=3$  atomic transition. About 8 mW power of this light is divided into three orthogonal and retroreflected beams to supply the three-dimensional

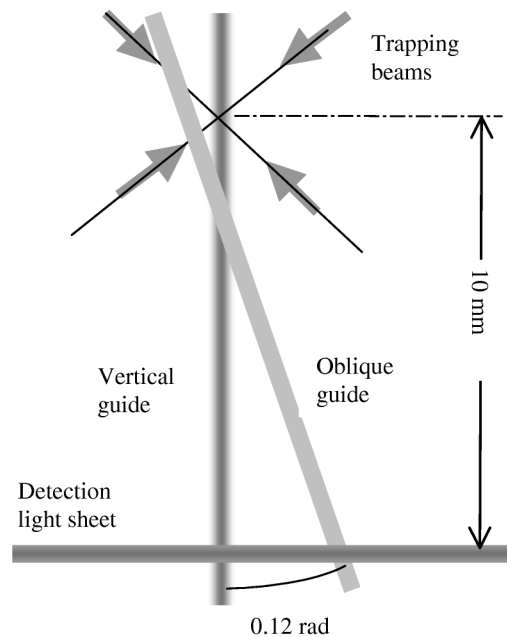


FIG. 1. Experimental scheme. The MOT is represented by four trapping beams. The others beams and the coils are omitted.

cooling setup. The repumping beam, provided by a free running laser diode tuned to  $5S_{1/2}F = 1 \rightarrow 5P_{3/2}F' = 2$  rubidium line, is superimposed to the trapping one. About 6 mW power is used. Cold atoms are first loaded in the MOT during 3 s with a trapping laser at a  $-2\Gamma$  frequency detuning ( $\Gamma$  being the natural linewidth of  $5P$  state). Then, with a sequence including a MOT at a  $-10\Gamma$  frequency detuning during 10 ms and a molasses regime during 10 ms, about  $10^7$  trapped atoms are cooled down to  $14 \mu\text{K}$ .

The dipole guides are realized by two intense far red-detuned laser beams, provided by a 15 W power TEM<sub>00</sub> CW Nd:YAG laser. The laser frequency detuning is about  $-10^7 \Gamma$ . With typical 0.1 mm sized beams it guarantees a spontaneous emission rate less than 0.1 photon/sec. No heating process occurs during the experiment, which is an essential ingredient to preserving the atoms in the guides.

The vertical guide is done with 14 W of the Nd:YAG laser. The beam dimension is 0.2 mm ( $1/e^2$  radius). Over the analysis region, which is 10 mm long, the beam size varies only by 5%. The guide can thus be considered a parallel one. The depth of the corresponding two-dimensional potential well is  $U_v = 30 \mu\text{K}$ .

When the trapping and repumping lasers are switched off, the atoms fall due to gravity. About 10% of them are kept inside the vertical guide. Studies about atom guiding by laser can be found in Refs. [15–17]. We let fall the atoms into the vertical guide during a time  $t_{\text{fall}}$ . We denote  $z_c$  the corresponding mean fall distance. At this moment the oblique guide is switched on suddenly. In our device, the oblique guide is switched on when the atomic cloud reaches the region of the 2-guides intersection. With this timing sequence the atoms are first coupled to the vertical guide and then the atomic cloud is split by the second guide. It prevents atoms of the initial trap from being captured by the oblique guide.

The oblique guide consists of a 0.3 mm waist beam, with a 10 W power, obtained by reflecting and refocusing the vertical beam as it goes out of the vacuum chamber. The corresponding two-dimensional potential depth is  $U_0 = 10 \mu\text{K}$ . Previous Monte Carlo simulations, taking into account the experimental geometry, have determined the optimum coupling to occur at an angle of  $0.12(1)$  rad which is then employed in the experiment. The intersection position,  $z_i$ , is controlled via a vertical translation of the mirror which defines the oblique guide.

The oblique guide is switched on and off with a mechanical shutter with a switching time less than  $500 \mu\text{s}$ . The oscillation frequency of the atoms in the vertical guide is about 100 Hz and their mean longitudinal velocity ranges 0.2 to 0.3 m/s at the 2-guides intersection, a few millimeters below the trap. The intersection region being about 5 mm high, the atoms oscillate once in the guide overlap region. The time variation of the potential can be considered sudden.

The splitting effect is analyzed 10 mm below the MOT center by imaging the atomic cloud (see Fig. 1). The observation direction is perpendicular to the plane of the guides. A weak resonant light sheet, 1 mm thick, slightly red detuned, retroreflected, and linearly  $\perp$  linearly polarized, induces the atom fluorescence in a 1-dimensional optical molasses, and, permits a correct imaging without any transverse atom displacement. The detection device, which uses a cooled CCD camera, is sensitive enough to perform single shot experiments [18]. Three pictures are recorded for each set of parameters: one without any guide, one with the vertical guide, and the last one with the two guides. Making numerical differences of the images, the atom transfer can be deduced.

Figures 2(a) and 2(b) show such image differences. Figure 2(a) has been recorded with only the vertical guide on. Figure 2(b), obtained using the two guides, for  $t_{\text{fall}} = 29$  ms ( $z_c = 4$  mm), clearly demonstrates the splitting effect. The two atomic clouds are  $\sim 1$  mm apart. The pictures represent the fluorescence of the atoms in the guide and do not represent the atomic density. The density measurement, and therefore the splitter efficiency and the dimensions of the two clouds, requires an analysis taking into account the change in the fluorescence rate of atoms located in the guides. The energy levels of the atoms being light shifted due to the intense light of the guiding beams, atoms in the middle of the beams emit less photon than those located at their borders. Therefore, the atomic peak density should be higher than one we naively get from the image. A correct analysis requires a good knowledge of the guiding beam. For that purpose, profiles of the guide beam have been scanned, checking the Gaussian shape and the waist dimension.

Figure 3 presents atomic density profiles deduced from picture cross-sections at the middle of the detection light sheet. The modification of the fluorescence rate due to the light shift has been included. We have also subtracted the contribution of the unguided atoms and of the background atoms. Figure 3(c) is the numerical difference of

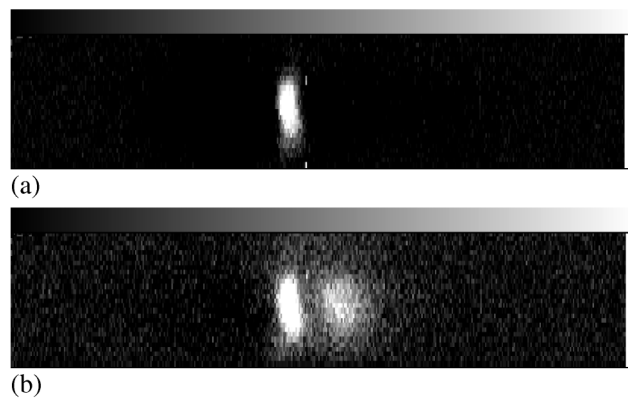


FIG. 2. Pictures of the cloud, imaged in the probe beam, for the vertical guide (a) and for two guides (b). The zero-guide image has been subtracted. The picture size is  $7.2 \text{ mm} \times 0.6 \text{ mm}$ .

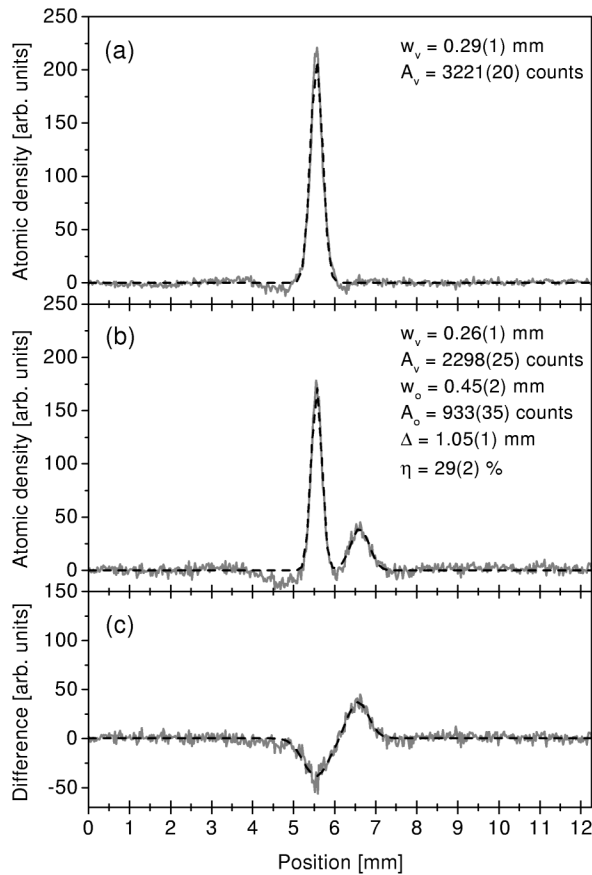


FIG. 3. Atomic density cross-sections (gray lines), for the vertical guide (a) and for two guides (b) for  $z_c = 4$  mm and  $z_i \sim 2$  mm. The background signal due to nonguided atoms has been subtracted. Figure (c) is the difference of (b) and (a). Dashed lines are fitting curves using two Gaussian functions,  $A_v$  and  $A_o$ , being the areas,  $w_v$  and  $w_o$  the  $1/e^2$  radius,  $\Delta$  the peak separation, and  $\eta$  the efficiency.

the Fig. 3(b) and Fig. 3(a) signals. The atom number is checked to be constant by comparing the peak areas in Figs. 3(a) and 3(b). As shown by the plot of Fig. 3(c), the atoms missing in the vertical guide have been integrally transferred to the oblique guide.

The beam-splitter efficiency is measured by analyzing the data of Fig. 3(b). The peak areas,  $A_v$  for atoms in the vertical guide and  $A_o$  for the oblique guide, provide the efficiency  $\eta = A_o/(A_v + A_o) = 29(2)\%$  in this case.

The distance between the two atomic clouds, measured to be  $\Delta = 1.05(1)$  mm, is larger than the width of the clouds themselves. It leads to a true separation of the clouds. It is one of the promising properties of the beam splitter, not only for a large area interferometer, but also for the use of one of its arms for phase-shift measurements. Because of the 0.12 rad angle, the splitting measurement  $\Delta$  gives the position of the guide intersection. We find in this case that the guide intersection is located 8 mm above the detection light sheet, corresponding to  $z_i = 2$  mm. With  $t_{fall} = 29$  ms ( $z_c = 4$  mm), we find

that  $z_i - z_c = -2$  mm, i.e., the intersection position does not correspond exactly to the cloud center after a 29 ms time of flight. It indicates that, even if the overlap of the guides is not maximum at the cloud position, an efficient transfer occurs.

The width of the clouds is deduced from analysis of Fig. 3. In the cases of Figs. 3(a) and 3(b) the cloud widths are larger than the dipole guide dimensions by a  $\sim 1.5$  ratio. Such a result has already been observed and discussed in the case of a single guide experiment [16]. For the oblique guide cloud,  $w_o = 0.45(2)$  mm leads also to a 1.5 ratio. It indicates that the atomic density cannot be described with the Maxwell-Boltzmann statistics.

In order to study the beam splitter coupling versus the distance  $z_i - z_c$ , we have recorded the atomic density by varying  $z_i$ ,  $z_c$  remaining the same. The evolution of the coupling is shown in Fig. 4 for  $z_i - z_c$  varying over a 20 mm range. The intersection position is evaluated by the mirror translation and is exactly measured from the distance between the two detected clouds. In the cases of truly separated clouds [Figs. 4(b)–4(f)], the efficiency is maximum,  $\eta = 44(3)\%$ , for  $z_i - z_c = 0.0(7)$  mm. As expected, the intersection position corresponds to the cloud altitude after a 29 ms time of flight. In Fig. 4(g) the overlap of the guides is quite large at the detection position and the obtained atomic density profile does not permit to measure correctly the beam splitter efficiency. This data provides directly the atomic density in the guide at the intersection. In this case the deduced  $\eta = 56(4)\%$  parameter represents the relative atom number in the oblique guide potential. This number has to be compared to the relative phase space accessible by the guides, which is given by  $U_0 w_0^2 / (U_0 w_0^2 + U_v w_v^2)$ . The parameters of the two-dimensional potentials gives 43(10)%, which is in agreement with the experimental observation.

For data of Figs. 4(a)–4(e),  $z_i - z_c$  is negative, indicating that the intersection is located above the cloud center after a 4 mm fall. In these cases, at the coupling time, the atoms are therefore submitted to a two-well potential. It is the sum of two Gaussian wells. With such shaped potential, the coupling is efficient even though the two potential minimums are separated by more than their width. Atoms having an energy higher than the energy barrier located between the two wells can access the oblique guide. The energy barrier provides an energy selective element of the beam splitter. In cases of Figs. 4(f) and 4(g) the barrier does not exist.

Furthermore, switching on the oblique guide rapidly, the atoms are submitted to a nonadiabatic potential variation. Those located at the vertical guide border with a small velocity can be coupled into the second guide, because they get a momentum kick due to the energy variation. Even if the spatial overlap of the two guides is small the potential energy is modified as a stair, giving a tiny acceleration, large enough to drive atoms into the next well. The time variation of the oblique guide should explain the

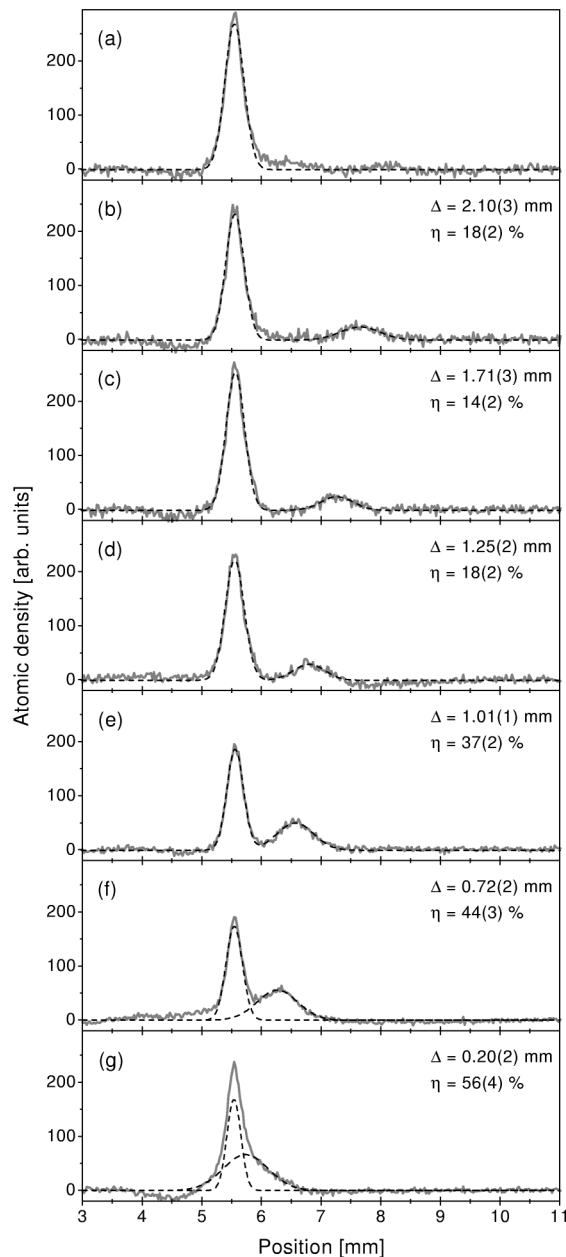


FIG. 4. Atomic density cross-sections (gray lines) for different intersection positions:  $z_i - z_c = -14.3(24)$  mm (a);  $z_i - z_c = -11.5(18)$  mm (b);  $z_i - z_c = -8.2(14)$  mm (c);  $z_i - z_c = -4.4(11)$  mm (d);  $z_i - z_c = -2.4(8)$  mm (e);  $z_i - z_c = 0.0(7)$  mm (f);  $z_i - z_c = 4.4(3)$  mm (g). The background signal due to nonguided atoms has been subtracted. Dashed lines are fitting curves using two Gaussian functions,  $\eta$  being the efficiency and  $\Delta$  the peak separation.

relative high efficiency we obtained in Figs. 4(b)–4(e). Indeed, with steady guides, we expect lower values. It explains also why we have observed up to 2 mm splittings [Fig. 4(b)].

As a consequence, in the two-well potential case the atoms which rest in the vertical guide should become colder. A further study of the atom velocity distribu-

tion would be required to analyze the evaporative process. Moreover, the guided atom density being too low, no collision occurs in the vertical guide, the atomic cloud cannot be thermalized, and a decrease of the cloud width could not be observed clearly. In another shaped beam, this process could become efficient.

In summary, we have demonstrated an efficient atomic beam splitter realized with two intense crossing detuned light beams. The beam splitter allows us to separate atoms with a large angle separation of 0.12 rad, which produces a macroscopic separation of the two atomic beams. The separation is larger than the sizes of the atomic beams. The coupling of the atoms in the oblique guide being efficient, splitting is observed even if the overlap of the guides is not maximum. In that case, only atoms with higher energy are coupled into the oblique guide. Being energy selective, the beam splitter has great promise to evaporate atoms, either from a dipole trap, or from a magnetic trap. Because no spontaneous emission occurs in the guides, the beam splitter should preserve the coherence. The use of a coherent atomic source as a Bose-Einstein condensate would permit the possibility to test the coherence properties of such a beam splitter and then to perform an atomic interferometer with a large enclosed area in a reduced-size apparatus.

- 
- [1] *Atom Interferometry*, edited by P.R. Bernann (Academic Press, Boston, 1997).
  - [2] C. S. Adams, M. Sigel, and J. Mlynek, Phys. Rep. **240**, 143 (1994).
  - [3] F. Riehle *et al.*, Phys. Rev. Lett. **67**, 177 (1991).
  - [4] D. S. Weiss, B. C. Young, and S. Chu, Phys. Rev. Lett. **70**, 2706 (1993).
  - [5] T. Pfau *et al.*, Phys. Rev. Lett. **71**, 3427 (1993).
  - [6] M. Weitz, B. C. Young, and S. Chu, Phys. Rev. Lett. **73**, 2563 (1994).
  - [7] M. Weitz, T. Heupel, and T. W. Hänsch, Phys. Rev. Lett. **77**, 2356 (1996).
  - [8] M. J. Snadden *et al.*, Phys. Rev. Lett. **81**, 971 (1998).
  - [9] P. J. Martin *et al.*, Phys. Rev. Lett. **60**, 515 (1988).
  - [10] D. M. Giltner, R. W. McGowan, and S. A. Lee, Phys. Rev. A **52**, 3966 (1995); M. K. Oberthaler *et al.*, Phys. Rev. Lett. **77**, 4980 (1996).
  - [11] S. Kunze, S. Dürr, and G. Rempe, Europhys. Lett. **34**, 343, (1996).
  - [12] M. Kozuma *et al.*, Phys. Rev. Lett. **82**, 871 (1999).
  - [13] J. Denschlag *et al.*, Appl. Phys. B **69**, 291 (1999); D. Cassetari *et al.*, Appl. Phys. B **70**, 721 (1999).
  - [14] P. Rosenbusch *et al.*, Phys. Rev. A **61**, 031404(R) (2000).
  - [15] K. Szymaniec, H. J. Davies, and C. S. Adams, Europhys. Lett. **45**, 450 (1999).
  - [16] L. Pruvost *et al.*, Opt. Commun. **166**, 199 (1999).
  - [17] X. Xu, Y. Wang, and W. Jhe, J. Opt. Soc. Am. B **17**, 1039 (2000), and Refs. [13–17] therein.
  - [18] I. Serre, L. Pruvost, and H. T. Duong, Appl. Opt. **37**, 1016 (1998).